Available online at BCREC Website: http://bcrec.undip.ac.id

Bulletin of Chemical Reaction Engineering & Catalysis, 8 (1), 2013, 83 - 88

Research Article

Synthesis and Characterization of $Ag/Ce_{1-x}Mn_xO_{2-\delta}$ Oxidation Catalysts

David Alami *, Viktor Bulavin

Department of Inorganic Substances Technology, National Technical University "Kharkiv Polytechnic Institute", Kharkiv, 61002, Ukraine

Received: 2nd April 2013; Revised: 11st May 2013; Accepted: 24th May 2013

Abstract

The aim of this work was to obtain samples of Ag-doped manganese-cerium mixed oxides and explore their characteristics. Six catalysts were prepared by the co-precipitation process followed by impregnation method for Ag incorporation. These catalysts were characterized in particular by means of Transmission Electron Microscopy (TEM), X-ray Diffraction (XRD), Temperature Programmed Reduction (TPR), BET surface area, and examined on the reaction of hydrogen peroxide catalytic decomposition. The samples obtained were solid solution nanoparticle agglomerates with irregular surface morphology. The results pointed out that the highest activity in oxidation reactions should possess $Ag/Ce_{0.23}Mn_{0.77}O_{2-\delta}$ catalyst.

Keywords: Catalytic Activity; Catalyst Characterization; Coprecipitation; Mixed Oxide; Solid Solution

How to Cite: Alami, D., Bulavin, V. (2013). Synthesis and Characterization of $Ag/Ce_{1-x}Mn_xO_{2-\delta}$ Oxidation Catalysts. *Bulletin of Chemical Reaction Engineering & Catalysis*, 8 (1): 83-88. (doi:10.9767/bcrec.8.1.4718.83-88)

Permalink/DOI: http://dx.doi.org/10.9767/bcrec.8.1.4718.83-88

1. Introduction

The composition of the Mn–Ce mixed oxide catalysts completely determine the catalytic activity in oxidation reactions. The optimal composition was found to depend on the nature of the compound to be oxidized [1]. The redox properties of a catalyst can be estimated from the H_2O_2 catalytic decomposition reaction rate and by temperature programmed reduction (TPR) [2]. It is observed that the catalysts with high redox ability are quite effective in oxidation reactions. Consequently, redox properties of a catalyst are thought to be the most important factor controlling catalytic activity [3].

* Corresponding Author.
E-mail: david.alami@gmail.com (D. Alami)

Concerning the composition–activity relationships for a catalyst, several factors should be taken into account, such as textural, structural and redox properties. Ceria-containing materials have come under widespread practice as catalysts at present. When associated with transition metal oxides, cerium oxide was shown to promote oxygen storage and release, to enhance oxygen mobility, to create surface and bulk vacancies and to improve the catalyst redox properties of the composite oxide [4]. Addition of cerium oxide to manganese oxide in small amounts has been shown to affect remarkably the oxidation state of manganese. Noticeably, the addition of silver can significantly improve the catalytic activity [5].

In this study, MnO_x–CeO_2 mixed oxides prepared by coprecipitation method were further doped by promotional quantities of silver. The com-

position of solid solution formed is believed to be $Ag/Ce_{1-x}Mn_xO_{2-\delta}$, where δ depicts the oxygen vacancies in this nonstoichiometric solid oxide. The aim of this paper is a synthesis of $Ag/Ce_{1-x}Mn_xO_{2-\delta}$, characterization and testing its catalytic activity in hydrogen peroxide decomposition reaction .

2. Materials and Methods

2.1. Preparation of Catalysts

The series of catalysts were prepared by co-precipitation method. The precursors of the catalyst, namely, manganese nitrate $Mn(NO_3)_2.6H_2O$, cerium nitrate $Ce(NO_3)_3.6H_2O$, and silver nitrate $AgNO_3$ were purified from bi-distilled water by re-crystallization method. Aqueous ammonia $NH_3.H_2O$ was used as a precipitation agent without preliminary purification. The procedure of co-precipitation was as follows: 30% $NH_3.H_2O$ solution was slowly added with continuous stirring to a solution containing different quantities of $Mn(NO_3)_2.6H_2O$ and $Ce(NO_3)_3.6H_2O$ at 323 K until the pH value of the mixture reached 10.5 (eq.1-2).

$$Mn(NO_3)_2 + 2NH_3.H_2O \leftrightarrow Mn(OH)_{2(s)} + 2NH_4NO_3 \quad (1)$$

$$Ce(NO_3)_3 + 3NH_3.H_2O \leftrightarrow Ce(OH)_{3(s)} + 3NH_4NO_3 \quad (2)$$

The precipitate was further aged at 323 K for 2 h in the mother liquid. After filtration and washing with distilled water, the obtained solid was dried at 383 K during 12 h and calcined in the air at 573 K during 6 h (eq.3-4).

$$(1-x)Ce(OH)_{3(s)} + xMn(OH)_{2(s)} + (0.5x-\delta+0.5)O_2 \leftrightarrow Ce_{1-x}Mn_xO_{2-\delta(s)} + (1.5-0.5x)H_2O \quad (3)$$

$$NH_4NO_3 \leftrightarrow N_2O_{(g)} + 2H_2O \quad (4)$$

Silver loading of 0.64 wt.% was made by impregnation method. The $Ce_{1-x}Mn_xO_{2-\delta}$ powder was initially dispersed in aqueous solution of $AgNO_3$. After filtration the solid obtained was calcined in the air at 573 K during 6 h.

After the calcination all catalysts were mechanically crushed to a fine powder in order to provide maximum specific surface area. In that way powder catalysts $Ag/Ce_{1-x}Mn_xO_{2-\delta}$ with x=0.70; 0.75; 0.77; 0.80; 0.83; 0.85 were obtained. The calcined solids were characterized by different methods: X-ray Diffraction (XRD), optical and electronic microscopy and temperature programmed reduction.

2.2. Characterization of Catalysts

2.2.1. Transmission Electron Microscopy (TEM)

Transmission electron microscopy analysis of the catalysts was performed using a PHILLIPS CM12 Microscope (point-to-point resolution, 3 Å).

2.2.2. Surface Area (S_{BET})

The specific (Brunauer–Emmett–Teller) surface areas were determined using N_2 adsorption isotherms of the samples performed at 77 K using a Micromeritics ASAP 2000 analyzer. Specific surface areas were determined by using the linear portion of the BET plot. Prior to the measurement, the samples were degassed in a vacuum at 573 K for 2 h.

2.2.3. X-ray Diffraction (XRD)

XRD spectra were recorded by DRON-3M powder diffractometer using nickel-filtered CuKα radiation operating at 40 kV and 200 mA.

2.2.4. Temperature Programmed Reduction (TPR)

Temperature-programmed reduction measurements were carried out using an installation represented on Figure 1. Gases applied in work (H_2, He) (1,2) were purified from oxygen and moisture im-

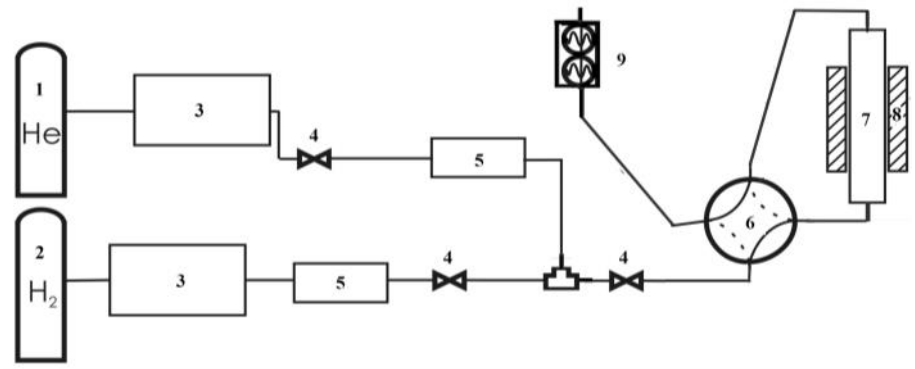

Figure 1. TPR measurement installation

purity as follows. Gas initial passes through Ni-Cr catalyst placed into the tube thermostatic (T = 523 K) reactor, where the gases were purified from oxygen impurity. Then gases come to absorbers filled with zeolite and silica gel where were further purified form moisture. Ultimate purification was reached by means of liquid nitrogen freezing (3). Mixing of gases in different quantities was carried out by electromagnetic valves (4), electronic regulators of a gas stream (5), and the four-way valve (6).

The TPR reactor (7) is a corrosion resistant stainless steel tube with the 130 mm length and inside diameter 5 mm. To prevent catalyst entrainment, both sides of a tube was packed with glass wool. Thermostatic control of the reactor was carried out by tube furnaces (8) connected to a TSD-detector which provided adjustment of the reactor temperature with accuracy of 1 K. The reactor temperature was controlled using a temperature control loop consisting of a thermocouple, a programmable temperature controller and the furnace heating element. About 50 mg of samples were loaded into the reactor and pretreated with He at 633 K for 2 h to remove the carbonates and hydrates adsorbed. After cooling down to the room temperature and introducing the reduction agent (5% H_2/He) with a flow rate of 50 mL/min, the temperature was then programmed to elevate in increments of 10 K/min up to 615 K.

2.2.5. Kinetic Measurements

Catalytic decomposition of hydrogen peroxide is the test reaction for catalytic activity determination. The process was performed at a constant temperature 293 K. For kinetic parameters determination the volume of gaseous oxygen was measured during the reaction time.

The solution of hydrogen peroxide with concentration 0.1 mole/dm^3 was used for experiments. The volume of hydrogen peroxide solution was 50 cm^3 and mass of the catalyst added was approximately 0.01 g. Volumetric measurements were performed on installation represented on Figure 2. A necessary quantity of catalyst was loaded into a funnel and washed off with known volume of hydrogen peroxide solution to the reactor (4) then the gauge-cock (2) turned off. Agitating and thermostatting has been reached with the use of a magnetic stirrer (5) with the thermo-controller. Oxygen which precipitates out during the decomposition process arrives through a tube (3) to burette for measuring the volume of gas (6) fixed on a support (7) and filled with water, and then water expelled to a funnel (8).

3. Results and Discussion

3.1. Structural and Morphological Properties

The results of TEM are illustrated by Figure 3. This figure shows the distribution of catalyst particle sizes and morphology. TEM picture of the representative catalyst shows that the system consists of large and "closely packed" agglomerates of "stepped" particles (~15 nm) with an irregular morphology. The composition effect on BET surface area is depicted in Table 1. The BET surface area increased monotonically with increasing contents of cerium, up to 45.6 m^2/g for the x = 0.8 sample, and then gradually dropped.

The XRD patterns of pure MnO_2, CeO_2 and Ag comparing to Ag/$Ce_{1-x}Mn_xO_{2-\delta}$ composite oxide catalysts are shown in Figure 4.

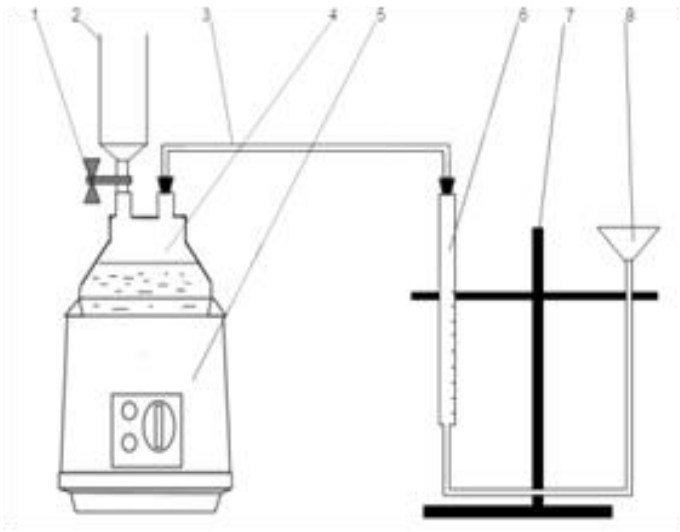

Figure 2. Volumetric measurement installation

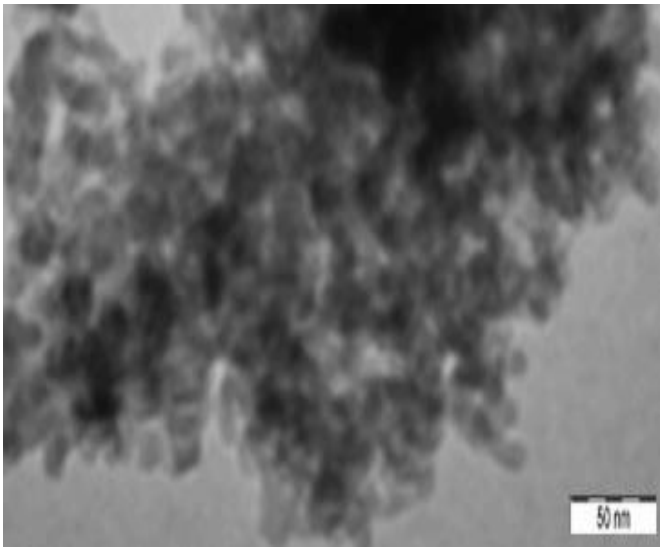

Figure 3. TEM micrograph of the catalyst

Table 1. BET surface area of the catalysts

$x(Ag/Ce_{1-x}Mn_xO_{2-\delta})$	S_{BET}, m^2/g
0.70	41.4
0.75	44.9
0.77	44.7
0.80	45.6
0.83	43.5
0.85	42.8

For the pure MnOx, the intensive and sharp diffractions at 2θ = 12.78, 18.08, 25.68, 37.48, 41.88 and 49.78 can be primarily attributed to MnO_2 (PDF #44-0141). In the XRD pattern of pure cerium oxide, the diffraction peaks at 2θ = 28.58, 33.08, 47.48 and 56.48 could be assigned to CeO_2 (PDF #43-1002). The diffraction peaks of MnO_2 and CeO_2 both appeared for the $Ag/Ce_{1-x}Mn_xO_{2-\delta}$ sample. As for the $Ag/Ce_{1-x}Mn_xO_{2-\delta}$ mixed oxides, the XRD pattern shows small diffraction of manganese oxides, but broad peaks due to CeO_2 of a cubic fluorite structure were observed. This is in good consistent with the recent report concerning the structure features of $Ce_{1-x}Mn_xO_{2-\delta}$ mixed oxides, which found that the phase composition of manganese and cerium mixed oxides strongly depended on the molar ratios of manganese and cerium oxides. The broad peaks in the diffraction pattern could be attributed to the formation of a solid solution between MnO_x and CeO_2. It can be further evidenced by the fact that the diffraction peaks of CeO_2 in the mixed oxide are slightly shifted to higher values of the Bragg angles, compared with the pure ceria. Since the ionic radius of Mn^{3+} (0.066 nm) is smaller than that of the Ce^{4+} (0.094 nm), the incorporation of Mn^{3+} into the ceria lattice to form MnOx–CeO_2 solid solution would result in remarkable decrease in the lattice parameter of ceria in the MnO_x–CeO_2 mixed oxide. For the $Ag/Ce_{1-x}Mn_xO_{2-\delta}$ catalysts, the intensive and sharp diffraction peaks could still be attributed to their corresponding supports, and no diffraction peaks due to the Ag_2O species could be observed. One can observe only discernable diffraction peaks at 2θ = 38.1, 44.3 and 64.4, which could be assigned to metal silver (PDF# 65-2871) .

3.2. Redox and catalytic properties

Depending on the surface areas, CeO_2 usually exhibited two reduction peaks at approximately 770 and 1100 K, which are ascribed to the reduction of surface and bulk oxygen of CeO_2, respectively. TPR profile of pure MnO_x showed two overlapped strong reduction peaks at 623–843 K with a slight shoulder at about 590 K [5]. It was proposed that the shoulder reduction peak of MnO_x was related to the readily reducible small cluster surface manganese species, and the two strong broad peaks correspond to the typical two-step reduction process of MnO_2: the first step involves the reduction of MnO_2 to Mn_3O_4, and the second step represents the reduction of Mn_3O_4 to MnO [7].

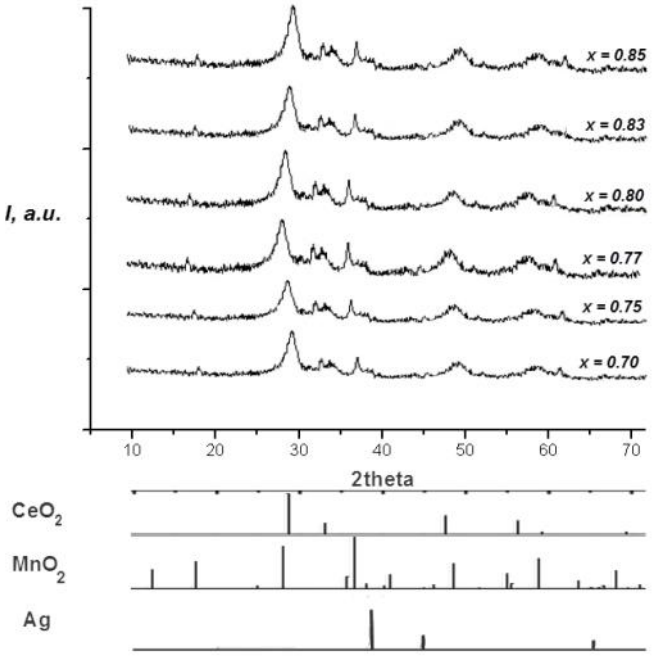

Figure 4. XRD pattern of the catalysts

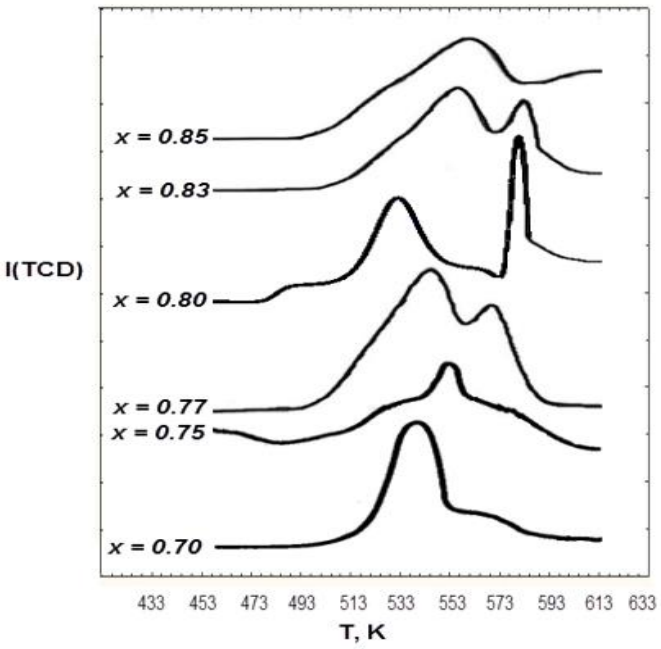

Figure 5. TPR pattern of the catalysts

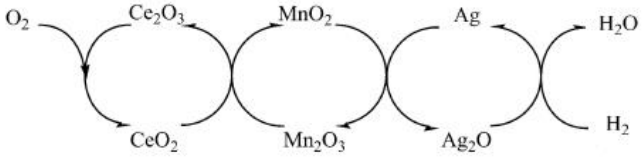

Figure 6. Oxygen transfer mechanism [7]

Compared to the reduction features of pure MnO_x and CeO_2, the reduction temperatures of the $Ag/Ce_{1-x}Mn_xO_{2-\delta}$ mixed oxide systematically shifted to lower regions (Figure 5). For the sample x = 0.8 two reduction peaks located at about 533 and 595 K can be clearly observed and correspond to the least reduction temperatures among the catalysts tested. The low temperature reduction peak could be attributed to the reduction of MnO_2 to Mn_3O_4, and the high-temperature reduction peak was assigned to the reduction of Mn_3O_4 to MnO together with the reduction of surface CeO_2.

The decrease of the reduction temperature indicated that the reduction of manganese and cerium oxides was promoted due to the synergetic interaction between manganese and cerium oxides through the formation of solid solution in which the mobility of oxygen species was greatly enhanced. As a matter of fact, this interaction can be interpreted in terms of an oxygen transfer mechanism relating to the oxygen mobility through the redox cycles of Ag^+/Ag^0, Mn^{4+}/Mn^{3+} and Ce^{4+}/Ce^{3+}, as shown below (Figure 6).

Presumably, the easy reduction of the $Ag/Ce_{1-x}Mn_xO_{2-\delta}$ catalyst leads to the easier activation and conversion of the oxygen species between the $Ce_{1-x}Mn_xO_{2-\delta}$ solid solution and the surface silver species, and consequently results in the higher catalytic activity. Obviously, the presence of silver noticeably shifted the reduction temperatures to lower values, indicating the existence of metal–support interaction between silver and $Ce_{1-x}Mn_xO_{2-\delta}$. This phenomenon can be explained in terms of the activation and spillover of oxygen from silver to manganese and cerium oxides, together with improving their reduction.

Initially, the oxygen species released from the decomposition of Ag_2O participated in the oxidation, and the re-oxidation of Ag to Ag_2O would be achieved via the oxygen species from MnO_2. Concurrently, the regeneration of the produced Mn_2O_3 to MnO_2 would be accomplished via the oxygen species from the oxygen storage of CeO_2, and the Ce_2O_3 thus formed can be re-oxidized into CeO_2 by the oxygen. This proposed oxygen transfer mechanism can be evidenced by earlier observations. Imamura has found that cerium oxide, based on its well-known oxygen storage capacity, could provide

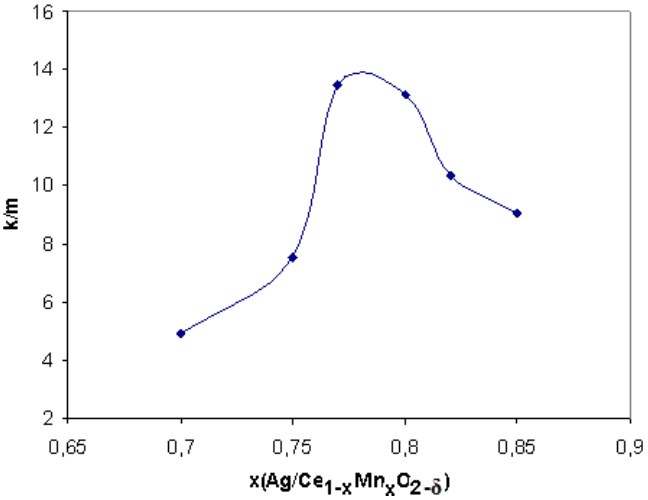

Figure 7. Effect of $Ag/Ce_{1-x}Mn_xO_{2-\delta}$ catalyst composition on hydrogen peroxide decomposition kinetics. Dependent variable is a kinetic constant reduced to catalyst loading

oxygen to MnO_x for increasing the valence of manganese in $Ce_{1-x}Mn_xO_{2-\delta}$ mixed oxide. It was also reported that manganese oxide could supply oxygen to the silver on the surface of an Ag/MnO_x catalyst so that the oxidation state of silver could be maintained [8]. Hence, transfer of oxygen from the oxygen reservoir CeO_2 to the active sites of Ag_2O through the MnOx can effectively facilitate the activation of molecular oxygen. The oxygen activation and its transfer between the support and the active metal should be strongly dependent on the redox properties of the catalyst. As a matter of fact, the extremely high catalytic activity of the $Ag/Ce_{1-x}Mn_xO_{2-\delta}$ catalyst is in good accordance with its reduction at much lower temperatures as shown in the TPR profiles. That is, the reduction behavior is intimately related to the catalytic performance of the $Ag/Ce_{1-x}Mn_xO_{2-\delta}$ catalyst.

The outcome of the hydrogen peroxide catalytic decomposition experiment has shown that the catalytic activity increased monotonically with an increase of Mn content up to x = 0.78. With the further manganese content increasing we observed catalytic activity decreasing (Fig. 7).

Calculations of the reaction order and kinetic constants were performed taking into account that the amount of oxygen released is proportional to the hydrogen peroxide conversion degree. The analysis of kinetic curves has led to the first order reaction kinetics. As seen in Figure 7, the most active catalyst is $Ag/Ce_{1-x}Mn_xO_{2-\delta}$ (x = 0.77).

4. Conclusions

In this investigation has provided synthesis, characterization and catalytic activity estimation of $Ag/Ce_{1-x}Mn_xO_{2-\delta}$ heterogeneous catalysts. The characterization by given physicochemical methods proved that the obtained samples are of great homogeneity and crystallinity. The catalytic activity tests carried on the six $Ag/Ce_{1-x}Mn_xO_{2-\delta}$ catalyst samples using hydrogen peroxide decomposition reaction. Structure analysis by XRD and TPR measurements disclosed that higher oxidation state of manganese and richer lattice oxygen species on the surface generated by the formation of $Ce_{1-x}Mn_xO_{2-\delta}$ solid solution which could enhance the activation of molecular oxygen through the oxygen transfer mechanism. The consecutive transfer of oxygen from the oxygen storage CeO_2 to the active center Ag_2O through MnO_x probably facilitates the complete oxidation reactions.

Acknowledgements

We should like to acknowledge the essential assistance of professors and PhD students of Pissarzhevsky Institute of Physical Chemistry (National Academy of Sciences, Ukraine). This research project would not have been possible without the support of these people.

References

[1] Chen, H., Sayari, A., Adnot, A. Larachi, F. (2001). Composition-activity effects of MnCeO composites on phenol catalytic wet oxidation. *Applied Catalysis B: Environmental*, 32(3):195-204.

[2] Imamura, S., Okumura, Y., Nishio, T., Utani, K. (1998). Wet-Oxidation of a Model Domestic Wastewater on a Ru/Mn/Ce Composite Catalyst. *Industrial & Engineering Chemistry Research*, 37(3): 1136-1139.

[3] Imamura, S. (1999). Catalytic and Noncatalytic Wet Oxidation. *Industrial & Engineering Chemistry Research*, 38(1): 1743-1753.

[4] Ding, Z., Li, L., and Wade, D. (1998). Supercritical Water Oxidation of NH_3 over a MnO_2/CeO_2 Catalyst. *Industrial & Engineering Chemistry Research*, 37(5): 1707-1716.

[5] Arena, F., Trunfio, G., Negro, G., Spadaro, L. (2008). Optimization of the $MnCeO_x$ system for the catalytic wet oxidation of phenol with oxygen (CWAO). *Applied Catalysis B: Environmental*, 85(1): 40-47.

[6] *The International Centre for Diffraction Data*, URL http://www.icdd.com.

[7] Tang, X., Chen J., Li, Y., Xu, Y., Shen, W. (2006). Complete oxidation of formaldehyde over Ag/MnO_xCeO_2 catalysts. *Chemical Engineering Journal*, 118: 119-125.

[8] Imamura, S., Shono, M., Okamoto, N., Hamada, A., Ishida, S. (1996). Effect of cerium on the mobility of oxygen on manganese oxides. *Applied Catalysis A: General*, 142(2): 279-288.